Progress In Electromagnetics Research B, Vol. 17, 69–84, 2009

A PLANT GROWTH SIMULATION ALGORITHM FOR PATTERN NULLING OF LINEAR ANTENNA ARRAYS BY AMPLITUDE CONTROL

K. Guney

Department of Electrical and Electronics Engineering
Faculty of Engineering
Erciyes University
Kayseri 38039, Turkey

A. Durmus

Department of Electrical and Electronics Engineering
Institute of Science and Technology
Erciyes University
Kayseri 38039, Turkey

S. Basbug

Department of Industrial Electronics
Vocational College
Nevsehir University
Nevsehir, Turkey

Abstract—A method based on plant growth simulation algorithm (PGSA) is presented for pattern nulling by controlling only the element amplitudes of linear antenna array. The PGSA is a new and highly efficient random search algorithm inspired by the growth process of plant phototropism. Simulation results for Chebyshev patterns with the imposed single, multiple and broad nulls are given to show the performance of the proposed method.

1. INTRODUCTION

Due to the increasing pollution of the electromagnetic environment, the antenna array, which allows placing nulls in the far field pattern at prescribed directions, is becoming important in radar, sonar and

Corresponding author: K. Guney (kguney@erciyes.edu.tr).

many communication systems for maximizing signal-to-interference ratio. Pattern nulling techniques available in the literature [1–20] include controlling the amplitude-only, the phase-only, the position-only, and the complex weights of the array elements. Interference suppression with complex weights is the most efficient because it has greater degrees of freedom for the solution space [1, 7]. On the other hand, it is also the most expensive considering the cost of both phase shifter and variable attenuator for each array element. Furthermore, when the number of elements in the antenna array increases, the computational time to find the values of element amplitudes and phases will also increase. The amplitude-only control [3, 7, 8, 12, 15, 17–19] uses a set of variable attenuators to adjust the element amplitudes. If the element amplitudes possess even symmetry about the center of the array, the number of attenuators and the computational time are halved. The problem of phase-only and position-only nulling is inherently nonlinear and it can not be solved directly by analytical methods without any approximation. By assuming that the phase or position perturbations are small, the nulling equations can be linearized. The phase-only control [4, 6, 10, 14, 16] utilizes the phase shifters while the position-only control [5, 6, 9] needs a mechanical driving system such as servomotors to move the array elements. Phase-only null synthesizing is less complicated and attractive for the phased arrays since the required controls are available at no extra cost, but it has still common problem.

In this paper, an alternative method based on plant growth simulation algorithm (PGSA) [21] is presented to place the single, multiple and broad nulls to the interference directions by controlling only the element amplitudes. The PGSA is based on the plant growth process, where a plant grows a trunk from its root; and some branches will grow from the nodes on the trunk; and then some new branches will grow from the nodes on the branches. The PGSA was successfully applied to solve various kinds of engineering problems [21–31]. The results showed that the performance of PGSA is better than that of genetic, tabu search and particle swarm optimization algorithms.

2. PROBLEM FORMULATION

If the element amplitudes are symmetrical about the center of the linear array, the far field array factor of this array with an even number of isotropic elements ($2N$) can be expressed as

$$AF(\theta) = 2 \sum_{n=1}^{N} a_n \cos\left(\frac{2\pi}{\lambda} d_n \sin\theta\right) \tag{1}$$

where a_n is the amplitude of the nth element, θ is the angle from broadside, and d_n is the distance between position of the nth element and the array center. Generally, the main beam of the array pattern is required to be directed to the desired signal and the undesired interference signals from other directions to be suppressed as much as possible. The main objective of PGSA proposed here is to find an appropriate set of required element amplitudes (a_n) that achieve interference suppression. To find a set of a_n values which produce the array pattern with nulls at any prescribed directions, the PGSA is used to minimize the following cost function.

$$g = \sum_{\theta=-90^\circ}^{90^\circ} W(\theta) \, |F_o(\theta) - F_d(\theta)| \tag{2}$$

where $F_o(\theta)$ and $F_d(\theta)$ are, respectively, the pattern obtained by using PGSA and the desired pattern. $W(\theta)$ is included in the cost function to control the null depth level. The value of $W(\theta)$ should be selected by experience such that the cost function is capable of guiding potential solutions to obtain satisfactory array pattern performance with desired properties. The factor $W(\theta)$ gives the antenna designer greater flexibility and control over the actual pattern. The trade-off of the relative importance between null depth and sidelobe level can easily be obtained by changing the value of the factor $W(\theta)$.

3. PLANT GROWTH SIMULATION ALGORITHM

The PGSA is based on the process of plant growth, in which a trunk grows from the root of the plant; and a number of branches grow from the nodes on the trunk; and then some new branches grow from the nodes on the branches [21–31]. This process continuously repeats itself until a plant is formed. Inspired by the analogy with the plant growth process, an optimization algorithm can be described. The system that is to be optimized first 'grows' by beginning at the root of a plant and then keeps 'growing' branches until the optimal solution is found.

3.1. The Growth Laws of a Plant

The following facts have been proved by the biological experiments about the growth laws of a plant,

(1) If the morphactin concentration of a node is high, the probability to grow a new branch on the node is high.

(2) The morphactin concentration of any node on a plant is not available in advance and is not constant; it is determined by

the environmental information of the node. The environmental information of a node is dependent on its relative position on the plant. The morphactin concentrations of all nodes of the plant are assigned depending on the new environment information after a new branch is grown.

3.2. Probability Model of Plant Growth

A probability model has been established by simulating the growth process of plant phototropism [21]. In this model, a function $g(\mathbf{Y})$ is defined to describe the environment of the node $\mathbf{Y}$ on a plant. The smaller the value of $g(\mathbf{Y})$ is, the better the environment of the node $\mathbf{Y}$ for growing a new branch is. The main outline of the model can be explained as follows: Initially, a plant grows a trunk M from its root $\mathbf{B}_0$. If we assume that there are k nodes $\mathbf{B}_{M1}, \mathbf{B}_{M2}, \ldots, \mathbf{B}_{Mk}$ having better environment than the root $\mathbf{B}_0$, on the trunk M, meaning that the function $g(\mathbf{Y})$ of the nodes $\mathbf{B}_{M1}, \mathbf{B}_{M2}, \ldots, \mathbf{B}_{Mk}$, and $\mathbf{B}_0$ satisfy $g(\mathbf{B}_{Mi}) < g(\mathbf{B}_0)$ $(i = 1, 2, 3, \ldots, k)$, then the morphactin concentrations $C_{M1}, C_{M2}, \ldots, C_{Mk}$ of the nodes $\mathbf{B}_{M1}, \mathbf{B}_{M2}, \ldots, \mathbf{B}_{Mk}$ can be obtained by using the following equation.

$$\begin{cases} C_{Mi} = \dfrac{g(B_0) - g(B_{Mi})}{\Delta_1} \\ \qquad\qquad\qquad\qquad (i = 1, 2, \ldots, k) \\ \Delta_1 = \sum\limits_{i=1}^{k} g(B_0) - g(B_{Mi}) \end{cases} \tag{3}$$

The importance of Equation (3) is that the morphactin concentration of any node is dependent on the relative magnitude of the gap of the environmental functions between the root and the corresponding node in overall nodes, which actually gives the relationship between the morphactin concentration and the environment.

From Equation (3), we get $\sum_{i=1}^{k} C_{Mi} = 1$, which means that the morphactin concentrations $C_{M1}, C_{M2}, \ldots, C_{Mk}$ of the nodes

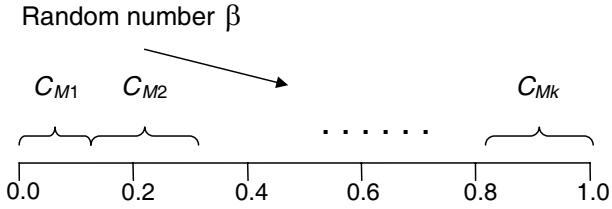

Figure 1. Morphactin concentration state space.

$\mathbf{B}_{M1}, \mathbf{B}_{M2}, \ldots, \mathbf{B}_{Mk}$ form a state space depicted in Fig. 1. If we select a random number β in the interval $[0, 1]$, then β will be like a ball thrown into the interval $[0, 1]$ and will drop into one of $C_{M1}, C_{M2}, \ldots, C_{Mk}$ in Fig. 1. In this way, the corresponding node, called the preferential growth node, will take priority of growing a new branch in the next step. In other words, $\mathbf{B}_{MT}$ will take priority of growing a new branch if the selected β satisfies $0 \leq \beta \leq \sum_{i=1}^{T} C_{Mi} (T = 1)$ or $\sum_{i=1}^{T-1} C_{Mi} < \beta \leq \sum_{i=1}^{T} C_{Mi} (T = 2, 3, \ldots, k)$. Let's suppose that the random number β drops into C_{M2}. This means that $\sum_{i=1}^{1} C_{Mi} < \beta \leq \sum_{i=1}^{2} C_{Mi}$. Then, the node $\mathbf{B}_{M2}$ will grow a new branch m. Assuming there are q nodes $\mathbf{B}_{m1}$, $\mathbf{B}_{m2}, \ldots, \mathbf{B}_{mq}$ having better environment than the root $\mathbf{B}_0$, on the branch m, their corresponding morphactin concentrations will be $C_{m1}, C_{m2}, \ldots, C_{mq}$. Now, not only the morphactin concentrations of the nodes on branch m need to be calculated, but also the morphactin concentrations of the nodes except $\mathbf{B}_{M2}$ (the morphactin concentration of the node $\mathbf{B}_{M2}$ becomes zero after it grows the branch m) on trunk M need to be recomputed after growing the branch m. The computation can be performed by employing Equation (4), which is derived from Equation (3) by adding the related terms of the nodes on branch m and discarding the related terms of the node $\mathbf{B}_{M2}$.

$$\begin{cases} C_{Mi} = \dfrac{g(\mathbf{B}_0) - g(\mathbf{B}_{Mi})}{\Delta_1 + \Delta_2} & (i = 1, 2, \ldots, k) \\ C_{mj} = \dfrac{g(\mathbf{B}_0) - g(\mathbf{B}_{mj})}{\Delta_1 + \Delta_2} & (j = 1, 2, \ldots, q) \\ \Delta_1 = \displaystyle\sum_{i=1, i\neq 2}^{k} (g(\mathbf{B}_0) - g(\mathbf{B}_{Mi})) \\ \Delta_2 = \displaystyle\sum_{j=1}^{q} (g(\mathbf{B}_0) - g(\mathbf{B}_{mj})) \end{cases} \tag{4}$$

It is also possible to derive $\sum_{i=1, i\neq 2}^{k} C_{Mi} + \sum_{j=1}^{q} C_{Mj} = 1$ from Equation (4). Now, the morphactin concentrations of the nodes (except $\mathbf{B}_{M2}$) on trunk M and branch m will form a new state space. A new preferential growth node that will grow a new branch in the next step can be gained in a similar way as $\mathbf{B}_{M2}$.

This process is repeated until there is no new branch to grow, which means that a plant is formed. From a mathematical point of view, the nodes in the plant can represent the possible solutions; $g(\mathbf{Y})$ can correspond to the objective function; the length of the trunk and the branch can correspond to the search domain of possible solutions; the root of a plant can represent the initial solution; and

the preferential growth node corresponds to the basic point of the next searching iteration.

The details on the PGSA can be found in [21–31]. In this paper, the PGSA described above is successfully used to optimize the antenna array element amplitudes to exhibit an array pattern with the imposed single, multiple and broad nulls.

4. NUMERICAL RESULTS

To show the performance of the proposed PGSA for steering single, multiple and broad nulls with the imposed directions by controlling the amplitude-only, four examples of a linear array with 20 isotropic elements have been performed. A 30-dB Chebyshev pattern given in Fig. 2 for 20 equispaced elements with $\lambda/2$ interelement spacing is utilized as the initial pattern.

It should be noted that the nodes on the trunk represent the element amplitudes. In this paper, addition to probability model of plant growth, we used a new selection method for node in which the new trunk will grow. In this selection method, new trunk grows from the node which has the best cost function value. This method is used to improve the local search ability.

The values of the cost function parameters given in (2) are selected as follows:

$$F_d(\theta) = \begin{cases} 0, & \text{for } \theta = \theta_i \\ \text{Initial pattern} & \text{elsewhere} \end{cases} \tag{5}$$

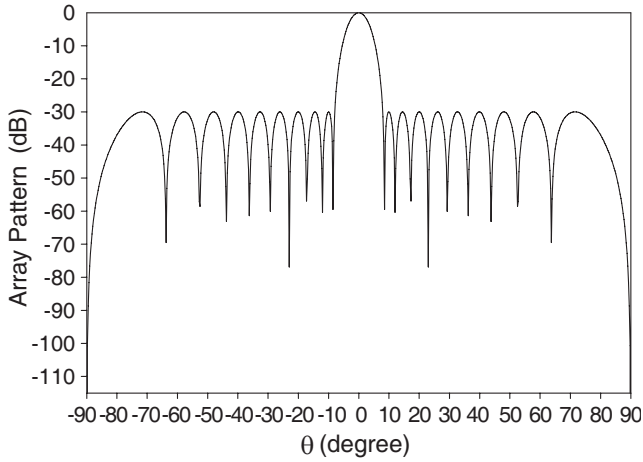

Figure 2. The initial 30-dB Chebyshev pattern.

and

$$W(\theta) = \begin{cases} 100, & \text{for } \theta = \theta_i \\ 1 & \text{elsewhere} \end{cases} \tag{6}$$

where θ_i is the direction of interference.

In the first, second and third examples, the Chebyshev patterns with a single null imposed at the direction of the second peak from

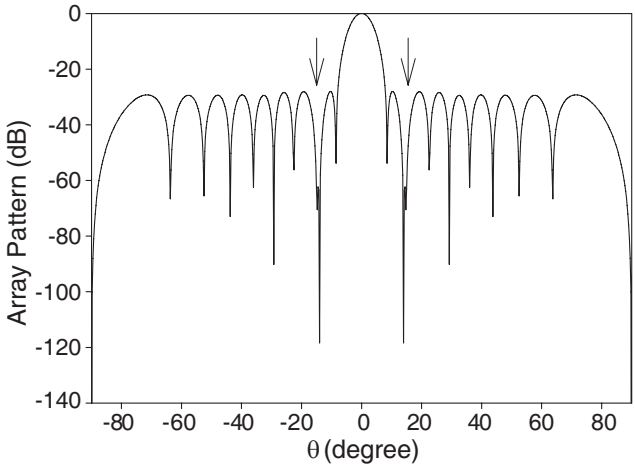

Figure 3. Radiation pattern with one imposed null at 14°.

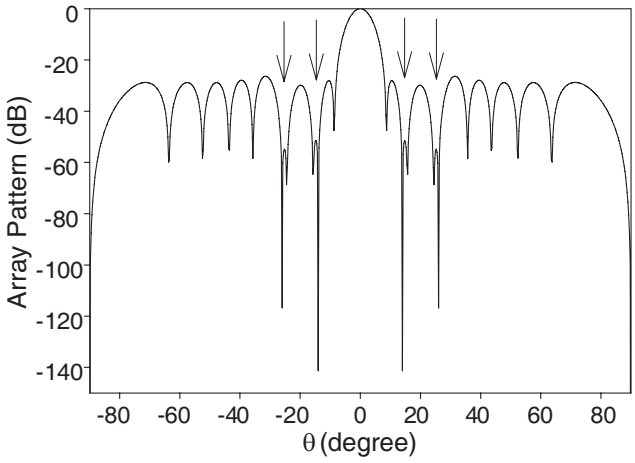

Figure 4. Radiation pattern with double imposed nulls at 14° and 26°.

Table 1. Element amplitudes normalized according to center elements for Figs. 3–6, and 11.

	Initial Chebyshev pattern	Computed with the PGSA				
k	Figure 2	Figure 3	Figure 4	Figure 5	Figure 6	Figure 11
±1	1.00000	1.00000	0.94885	1.00000	1.00000	1.00000
±2	0.97010	0.98665	1.00000	0.96227	0.98114	0.99547
±3	0.91243	0.95826	0.98908	0.98076	0.96261	0.97143
±4	0.83102	0.90187	0.86154	0.93835	0.88052	0.90942
±5	0.73147	0.79647	0.71832	0.75555	0.70638	0.80012
±6	0.62034	0.65347	0.63711	0.61563	0.57081	0.65405
±7	0.50461	0.49607	0.53316	0.57719	0.55623	0.49739
±8	0.39104	0.36049	0.35780	0.43113	0.48347	0.36269
±9	0.28558	0.25733	0.19995	0.20210	0.25470	0.26149
±10	0.32561	0.33716	0.30857	0.28367	0.25913	0.34535

main beam (14°), with double nulls imposed at the directions of the second and the fourth peaks from main beam (14° and 26°), and with triple nulls imposed at the directions of the second, fourth and fifth peaks from main beam (14°, 26°, and 33°) are considered. The

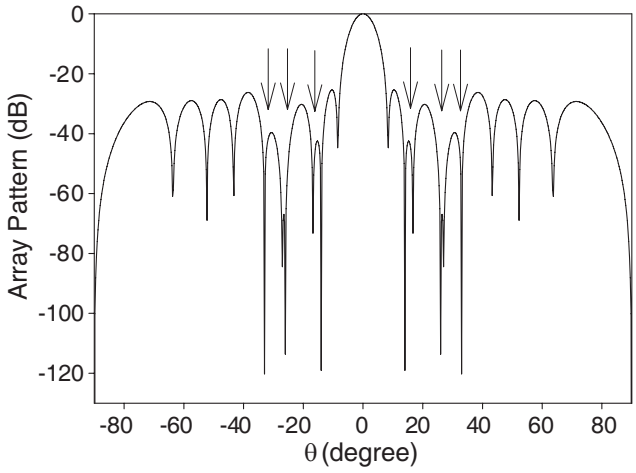

Figure 5. Radiation pattern with triple imposed nulls at 14°, 26°, and 33°.

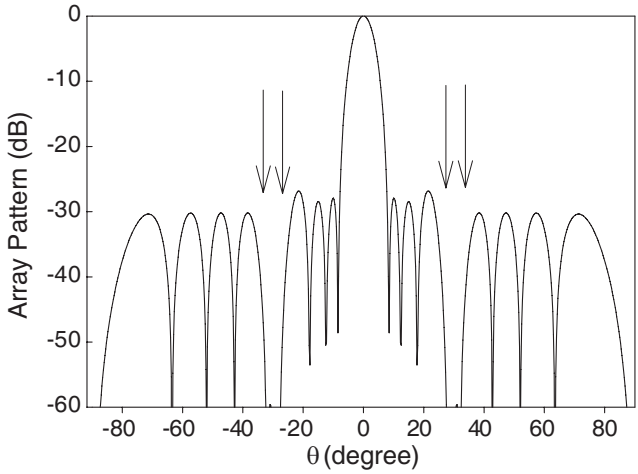

Figure 6. Radiation pattern with a broad null sector centered 30° with $\Delta\theta = 5°$.

resultant patterns are illustrated in Figs. 3–5. It can be seen from Figs. 3–5 that all desired nulls are deeper than −110 dB. In the fourth example, the pattern having a broad null located at 30° with $\Delta\theta = 5°$ is achieved and is shown in Fig. 6. From the figure, a null depth level deeper than −55 dB is obtained over the spatial region of interest. The element amplitude values normalized according to center elements for the patterns given in Figs. 3–6 are given in Table 1.

The results depicted in Figs. 3–6 demonstrate that the PGSA proposed in this paper can accurately obtain the nulling patterns by controlling only the element amplitudes of the linear array. From the null depth and the maximum sidelobe level points of view, the performances of the patterns are very good. The nulling technique based on PGSA preserves the characteristics of the initial Chebyshev pattern with little pattern disturbance except for the nulling directions. The half power beam width for nulling patterns obtained by the PGSA is almost equal to that of initial Chebyshev pattern.

Figure 7 shows the convergence curves of basic PGSA and the PGSA used in this paper. It is clear from Fig. 7 that the PGSA used in this paper leads to better convergence and that 800 iterations are needed to find the optimal solutions.

In Figs. 8–10, the results of PGSA are compared with the results of the modified touring ant colony optimisation (MTACO, see Fig. 6 in [8]), the bees algorithm (BA, see Fig. 4 in [17]), and the bacterial foraging algorithm (BFA, see Fig. 8 in [18]) for radiation pattern with

one null imposed at 14°. The null depth level (NDL), maximum sidelobe level (MSL), and dynamic range ratio (DRR = $|a_{\max}/a_{\min}|$) of the patterns obtained by using PGSA, MTACO, BA, and BFA are also given in Table 2. As can be seen, all of the four simulation

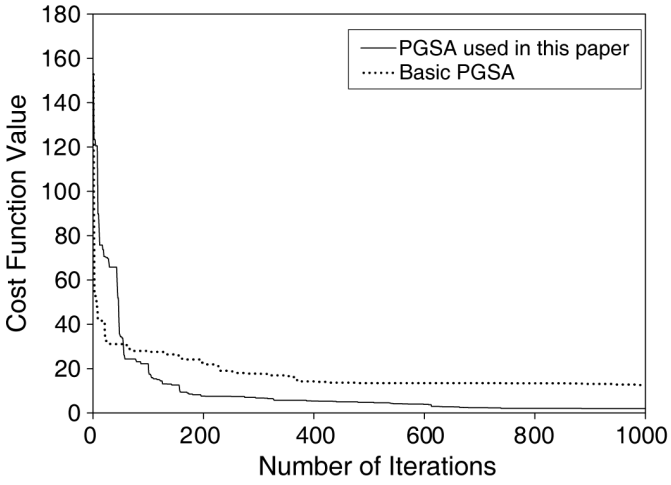

Figure 7. Convergence curve of the nulling pattern achived by the basic PGSA (dotted line) and the PGSA used in this paper (solid line).

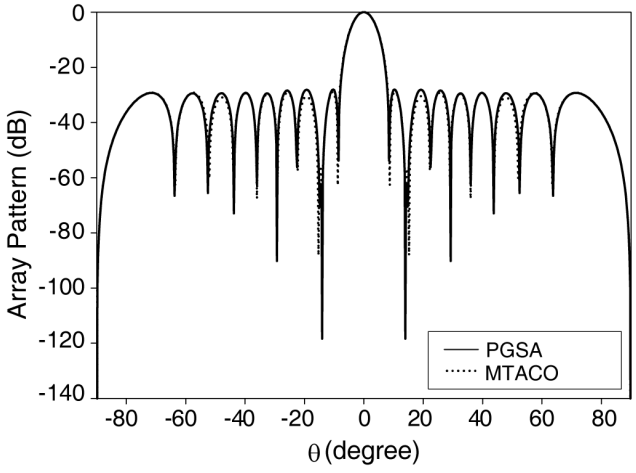

Figure 8. PGSA-optimized radiation pattern (solid line) with one null imposed at 14° in compassion with the result by MTACO (dotted line).

results agree well on the null positions, NDLs, and MSLs. There is a trade-off between the null depth level and maximum sidelobe level; usually, performance cannot be improved significantly for one without sacrificing the other. The restriction on the DRR can easily

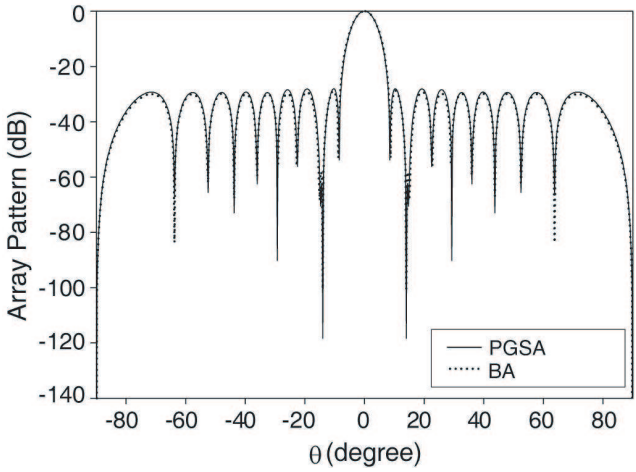

Figure 9. PGSA-optimized radiation pattern (solid line) with one null imposed at 14° in compassion with the result by BA (dotted line).

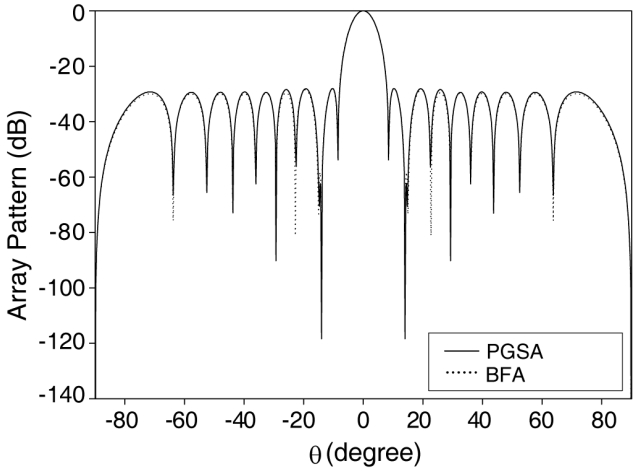

Figure 10. PGSA-optimized radiation pattern (solid line) with one null imposed at 14° in compassion with the result by BFA (dotted line).

Table 2. NDL, MSL, and DRR of the patterns in Figs. 3 and 8–10.

	Figure 3 (PGSA)	Figure 8 (MTACO)	Figure 9 (BA)	Figure 10 (BFA)
NDL (dB)	−118.3	−88.1	−100.4	−113.6
MSL (dB)	−28.03	−29.1	−28.8	−28.11
DRR	3.89	4.35	4.09	3.89

be achieved by suitably setting the search interval of amplitude weights. The smaller amplitude range means smaller degrees of freedom for the solution space hence worse sidelobe and null depth performance. The antenna designer should make a trade-off between the achievable and the desired pattern.

The simulation results for PGSA are obtained within 1–2 minutes on a personal computer with a Core Duo processor running at 1600 MHz. This is sufficient to produce satisfactory patterns with the desired performance on the average. The computation time can be significantly reduced by using faster computer systems. The PGSA can also be implemented in real time by using state-of-the art hardware devices, such as FPGAs (Field Programmable Gate Array). In this way, the computation time of the system is limited only by the response time of the FPGA, which is in the order of a few microseconds. The computation time of BFA [18] is almost the same as that of PGSA. The simulation results for BA [17] are obtained within 2–3 minutes on a personal computer with a Pentium 4 processor running at 2400 MHz. For MTACO [8], the calculations took almost 4–7 min on a personal computer with a Pentium 3 processor running at 750 MHz.

To show the flexibility of the PGSA, in the fourth example, it is intended to obtain a null depth level deeper than that of the first example. Thus, $W(\theta)$ is modified as given below while the values of other design parameters are the same as those of the first example.

$$W(\theta) = \begin{cases} 200, & \text{for } \theta = \theta_i \\ 1 & \text{elsewhere} \end{cases} \tag{7}$$

The corresponding pattern is shown in Fig. 11. The null depth level of the pattern in Fig. 11 is −137.1 dB while the null depth level of the pattern in Fig. 3 is −118.3 dB. But in response to such an improvement of the null depth level, the maximum sidelobe level of the pattern in Fig. 11 is −27.31 dB whereas that of the pattern in Fig. 3 is −28.03 dB. The results obtained here show that the null depth level and maximum sidelobe level of the nulling pattern can be easily adjusted by using PGSA. The element amplitude values normalized according to center element for the pattern given in Fig. 11 are given in Table 1.

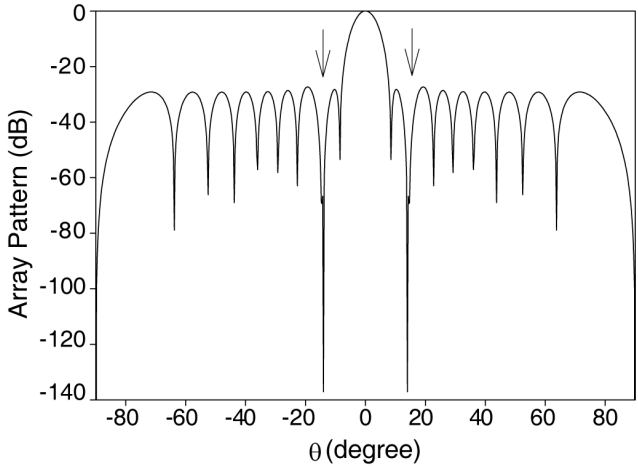

Figure 11. Radiation pattern with a null depth level deeper than that of the first example having one imposed null at 14°.

5. CONCLUSION

In this paper, a method based on PGSA for the pattern synthesis of linear antenna arrays with the prescribed nulls is presented. Nulling of the pattern is achieved by controlling only the element amplitudes. Numerical results show that the PGSA is capable of accurately determining the element amplitudes which yield the array patterns with single, multiple and broad nulls imposed at the directions of interference while the main beam and the sidelobes are quite close to the initial pattern. Although only linear antenna arrays have been considered here, the PGSA can easily be used for arrays with complex geometries as well as nonisotropic-elements. As an optimization algorithm, the PGSA will most likely be an increasingly attractive alternative, in the electromagnetics and antennas community, to other optimization algorithms.

REFERENCES

1. Steyskal, H., R. A. Shore, and R. L. Haupt, "Methods for null control and their effects on the radiation pattern," *IEEE Trans. Antennas Propagat.*, Vol. 34, 404–409, 1986.
2. Er, M. H., "Linear antenna array pattern synthesis with prescribed broad nulls," *IEEE Trans. Antennas Propagat.*, Vol. 38, 1496–1498, 1990.

3. Ibrahim, H. M., "Null steering by real-weight control — A method of decoupling the weights," *IEEE Trans. Antennas Propagat.*, Vol. 39, 1648–1650, 1991.
4. Haupt, R. L., "Phase-only adaptive nulling with a genetic algorithm," *IEEE Trans. Antennas Propagat.*, Vol. 45, 1009–1015, 1997.
5. Ismail, T. H. and M. M. Dawoud, "Null steering in phased arrays by controlling the element positions," *IEEE Trans. Antennas Propagat.*, Vol. 39, 1561–1566, 1991.
6. Liao, W. P. and F. L. Chu, "Array pattern nulling by phase and position perturbations with the use of the genetic algorithm," *Microwave and Optical Technology Letters*, Vol. 15, 251–256, 1997.
7. Guney, K. and A. Akdagli, "Null steering of linear antenna arrays using modified tabu search algorithm," *Progress In Electromagnetics Research*, PIER 33, 167–182, 2001.
8. Karaboga, N., K. Guney, and A. Akdagli, "Null steering of lineer antenna arrays by using modified touring ant colony optimization algorithm," *Int. J. RF and Microwave Computer Aided Eng.*, Vol. 12, 375–383, 2002.
9. Akdagli, A., K. Guney, and D. Karaboga, "Pattern nulling of linear antenna arrays by controlling only the element positions with the use of improved touring ant colony optimization algorithm," *Journal of Electromagnetic Waves and Applications*, Vol. 16, No. 10, 1423–1441, 2002.
10. Akdagli, A. and K. Guney, "Null steering of linear antenna arrays by phase perturbations using modified tabu search algorithm," *J. Communications Technology and Electronics*, Vol. 49, 37–42, 2004.
11. Khodier, M. M. and C. G. Christodoulou, "Linear array geometry synthesis with minimum sidelobe level and null control using particle swarm optimization," *IEEE Trans. Antennas Propagat.*, Vol. 53, 2674–2679, 2005.
12. Yang, S. W., Y. B. Gan, and A. Y. Qing, "Antenna-array pattern nulling using a differential evolution algorithm," *Int. J. RF and Microwave Computer Aided Eng.*, Vol. 14, 57–63, 2004.
13. Chung, Y. C. and R. L. Haupt, "Amplitude and phase adaptive nulling with a genetic algorithm," *Journal of Electromagnetic Waves and Applications*, Vol. 14, No. 5, 631–649, 2000.
14. Mouhamadou, M., P. Vaudon, and M. Rammal, "Smart antenna array patterns synthesis: Null steering and multi-user beamforming by phase control," *Progress In Electromagnetics*

Research, PIER 60, 95–106, 2006.

15. Babayigit, B., A. Akdagli, and K. Guney, "A clonal selection algorithm for null synthesizing of linear antenna arrays by amplitude control," *Journal of Electromagnetic Waves and Applications*, Vol. 20, No. 8, 1007–1020, 2006.
16. Mouhamadou, M., P. Armand, P. Vaudon, and M. Rammal, "Interference suppression of the linear antenna arrays controlled by phase with use of SQP algorithm," *Progress In Electromagnetics Research*, PIER 59, 251–265, 2006.
17. Guney, K. and M. Onay, "Amplitude-only pattern nulling of linear antenna arrays with the use of bees algorithm," *Progress In Electromagnetics Research*, PIER 70, 21–36, 2007.
18. Guney, K. and S. Basbug, "Interference suppression of linear antenna arrays by amplitude-only control using a bacterial foraging algorithm," *Progress In Electromagnetics Research*, PIER 79, 475–497, 2008.
19. Guney, K. and B. Babayigit, "Amplitude-only pattern nulling of linear antenna arrays with the use of an ımmune algorithm," *Int. J. RF and Microwave Computer Aided Eng.*, Vol. 18, 397–409, 2008.
20. Azevedo, J. A. R. and A. M. E. S. Casimiro, "Non-uniform sampling and polynomial interpolation for array synthesis," *IET Microw. Antennas Propag.*, Vol. 1, 867–873, 2007.
21. Tong, L., C. Wang, W. Wang, and W. Su, "A global optimization bionics algorithm for solving integer programming-plant growth simulation algorithm," *Systems Engineering-Theory & Practice*, Vol. 25, 76–85, 2005.
22. Wang, C. and H. Cheng, "Reactive power optimization based on plant growth simulation algorithm," *Power System Technology*, Vol. 30, 37–41, 2006.
23. Wang, C. and H. Cheng, "A plant growth simulation algorithm and its application in power transmission network planning," *Automation of Electric Power Systems*, Vol. 31, 24–28, 2007.
24. Wang, C. and H. Cheng, "Reconguration of distribution network based on plant growth simulation algorithm," *Proceedings of the CSEE*, Vol. 27, 50–55, 2007.
25. Wang, C. and H. Cheng, "Integrated optimization algorithm of dynamic reactive power for distribution system," *Transactions of China Electrotechnical Society,* Vol. 23, 109–114, 2008.
26. Luo, W., J. Yu, and J. Huang, "Bionic algorithm for solving nonlinear integer programming," *Computer Engineering and*

Applications, Vol. 44, 57–59, 2008.

27. Yang, L., K. Wang and X. Huang, "Application of trees growth simulation algorithm to solve reactive power optimization problem," *Journal of Zhengzhou University (Engineering Science)*, Vol. 29, 69–72, 2008.
28. Srinivasa, R. R. and S. V. L. Narasimham, "Optimal Capacitor placement in a radial distribution system using plant growth simulation algorithm," *Proceeding of World Academy of Science, Engineering and Technology*, Vol. 35, 716–723, 2008.
29. Wang, C. and H. Cheng, "Optimization of network configuration in large distribution systems using plant growth simulation algorithm," *IEEE Transactions on Power Systems*, Vol. 23, 119–126, 2008.
30. Tong, L. and W. Zhongtuo, "Application of plant growth simulation algorithm on solving facility location problem," *Systems Engineering-Theory & Practise*, Vol. 28, 107–115, 2008.
31. Wang, C. and H. Cheng, "Transmission network optimal planning based on plant growth simulation algorithm," *European Transactions on Electrical Power*, Vol. 19, 291–301, 2009.